Journal of Magnetic Resonance **136,** 143–151 (1999)
Article ID jmre.1998.1628, available online at http://www.idealibrary.com on IDEAL®

Analysis of *J* Coupling-Induced Fat Suppression in DIET Imaging

L. A. Stables,* R. P. Kennan,† A. W. Anderson,*,† R. T. Constable,† and J. C. Gore*,†

**Department of Applied Physics and †Department of Diagnostic Radiology, Yale University School of Medicine, New Haven, Connecticut 06520-8042*

E-mail: john.gore@yale.edu

Received November 6, 1997; revised September 25, 1998

The DIET (or *d*ual *i*nterval *e*cho *t*rain) sequence, a modification of the *f*ast *s*pin *e*cho (FSE) sequence that selectively reduces signal from fat in MR images, has been investigated. The DIET sequence uses an initial echo spacing longer than that of a conventional FSE sequence, thus allowing *J* coupling-induced dephasing to take effect. The sequence is evaluated theoretically, and its effectiveness on a hydrocarbon (1-pentene) is demonstrated numerically using density matrix calculations. The sequence is also evaluated experimentally using *in vitro* solutions and *in vivo* imaging. The efficacy of the sequence is compared for different lipid chemical structures, field strengths, and pulse sequence parameters.

Key Words: **fat suppression; *J* coupling; density matrix; numerical simulations; pulse sequence; DIET.**

INTRODUCTION

The signals from fat appear relatively brighter in *f*ast *s*pin *e*cho (FSE) images than in conventional *s*pin *e*cho (SE) images with comparable T_1 and T_2 weightings (*1–4*). The magnitude of the fat signal generally increases as the spacing between the 180° pulses decreases. This pulse spacing dependence results from changes in the effects of *J* coupling within the hydrocarbon chains of lipid molecules (*2, 5*). As the pulse spacings become shorter, the effects of *J* coupling disappear (*6*), and hence the lipid signal is enhanced relative to the surrounding tissue. It is often desirable to reduce the signal from fat selectively to achieve better contrast for detecting tissue abnormalities. However, the performances of conventional fat saturation techniques are often limited by the presence of B_0 and B_1 inhomogeneities. Recently a pulse sequence was developed which exploits *J* coupling-induced dephasing to reduce the lipid signal (*7, 8*). The sequence relies on the use of a longer echo spacing at the start of a FSE sequence. This permits *J* coupling effects to reduce the signals from fat while still allowing multiple echoes to be acquired in a relatively short time. In this paper we evaluate the efficacy of this technique, known as the *d*ual *i*nterval *e*cho *t*rain, or DIET, sequence, using theory and experiments on phantoms and report results using a DIET imaging sequence *in vivo.*

THEORY

Scalar *J* coupling can strongly influence the transverse signal decay in multipulse spin echo experiments (*6*). In hydrocarbon chains, *J* couplings arise largely from homonuclear interactions between neighboring protons. In homonuclear coupled systems, 180° pulses do not reverse the phase evolution caused by coupling between spins. As a result, the NMR signal is modulated in an oscillatory manner. For a simple doublet, when $J/\delta \ll 1$ and $\delta\tau > 1$ (where J is the coupling constant, δ is the absolute value of the chemical shift difference, and τ is the echo spacing), the echo train is modulated by $\cos(\pi n J\tau)$, where n is the echo number. For more complex spectra, the summation of modulated signals may appear more like a monotonically decreasing signal whose apparent T_2 is dominated by the number and strength of the couplings present, rather than simply the intrinsic relaxation time (*9*).

An equation characterizing the effect of *J* coupling in the Carr–Purcell spin echo sequence for different multiple spin systems has been derived using a density matrix formalism by Allerhand (*6*). Using this formalism, he showed that if the pulse spacing is small, such that the products $J_{jk}\tau$ and $\delta_{jk}\tau$ are $\ll 1$ for all j, k (where δ_{jk} is the chemical shift difference between spin groups j and k and J_{jk} is their coupling constant), then the effects of chemical shift disappear. This renders all of the spins magnetically equivalent and thus removes any dephasing effects. As a result, the equation governing the effects of *J* coupling in this regime reduces analytically to an expression independent of echo time. Figure 1 shows the effect of pulse spacing on the echo train of a hypothetical strongly coupled A_3B_2 system, with $J_{AB} = 6$ Hz and $\delta_{AB} = 40$ Hz. The echo train was evaluated numerically using Allerhand's formalism and omits intrinsic T_2 relaxation (*9*). The absolute value of the signal is given relative to its value immediately after the 90° pulse. When the pulse spacing, τ, is 4 ms, the echo train shows no modulation from *J* coupling, while in the $\tau =$ 10 ms echo train, the effects of *J* coupling cause a smoothly varying signal decay. As τ increases to 30 ms, oscillatory

1090-7807/99 $30.00

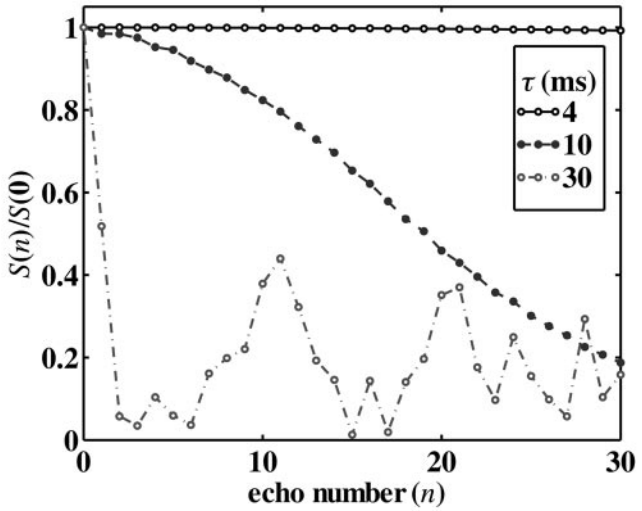

FIG. 1. The effect of J coupling on a strongly coupled A_3B_2 spin system. The plot shows signal vs echo number for CPMG sequences where τ, the spacing between echoes, is 4, 10, or 30 ms. $J_{AB} = 6$ Hz, $\delta_{AB} = 40$ Hz. Intrinsic T_2 relaxation is neglected. Note that as τ increases, J coupling becomes more effective at suppressing the NMR signal.

behavior enters the echo train, causing a faster initial decrease in signal intensity, as well as a nonmonotonic signal decay.

Using the density matrix formalism, one can show that the quantities which determine the strength of J-coupled dephasing are the products $\delta_{jk}\tau$, and $J_{jk}\tau$ (as opposed to the individual values of these parameters). Note that the J_{jk} coupling constants depend solely on the molecular properties of the lipid, whereas the δ_{jk} are determined by both the lipid electronic structure and the external magnetic field.

THE DIET SEQUENCE

The DIET sequence works by exploiting the dependence of fat signal on pulse spacing. In order to suppress J-coupled signals, the standard CPMG multiecho sequence is modified such that the spacing between the initial 90° pulse and the first echo is longer than the spacing between subsequent echoes. This allows a greater mixing of coupled spins during the first echo, which leads to dephasing and hence signal attenuation. A similar modification to the FSE imaging sequence was first suggested by Norris as a way of increasing the TE of an image; however, the potential for fat suppression with this sequence was not addressed (*10*). Figure 2 shows a schematic of the DIET sequence, where the parameters τ_1 and τ_2 refer to the time of the initial echo and the spacing of the following echoes, respectively. The advantage of this sequence for reducing the signal from fat over other techniques such as selective saturation is that it should be spatially uniform, since it is based on J coupling effects which are not subject to field inhomogeneities (*11*). However, the precise choice of timing parameters and the effectiveness of the sequence for different systems have not been previously investigated, nor has the validity of the sequence been demonstrated theoretically.

The density matrix formalism described in the previous section can also be applied to the DIET sequence, as is shown in the Appendix. We demonstrate there that in the limit of very fast pulsing in the second phase of the DIET sequence, the J modulation of the echo train disappears. Furthermore, the fat signal retains the suppression achieved during the first (τ_1) phase of the sequence. The pulse rates used in clinical FSE sequences fall short of the strict fast pulse requirement, which is that $|J_{jk}|\tau_2$ and $|\delta_j|\tau_2$ are $\ll 1$ for all j and k. However, when τ_2 is short but does not meet the fast pulse requirement, we expect that the DIET sequence should show a similar ability to retain the fat suppression achieved during the initial τ_1 period. We confirmed the validity of this hypothesis in computer simulations of the evolution of the density matrix during the DIET sequence.

SIMULATION AND PHANTOM STUDIES OF THE DIET SEQUENCE

Simulation Algorithm

The signal produced by using the DIET sequence on a given spin system was calculated by numerically solving the matrix equation from quantum mechanics (*12*)

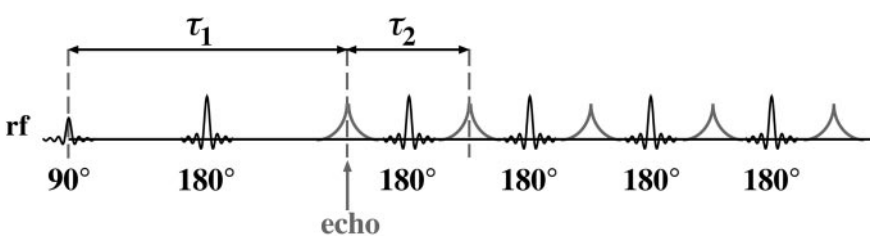

FIG. 2. The DIET pulse sequence. This sequence is a modification of the CPMG multiecho sequence, where the spacing between the initial 90° pulse and the first echo is longer than the subsequent echo spacing. The longer initial echo time allows more J coupling-induced spin dephasing to occur. The spins remain dephased even after the faster pulsing begins.

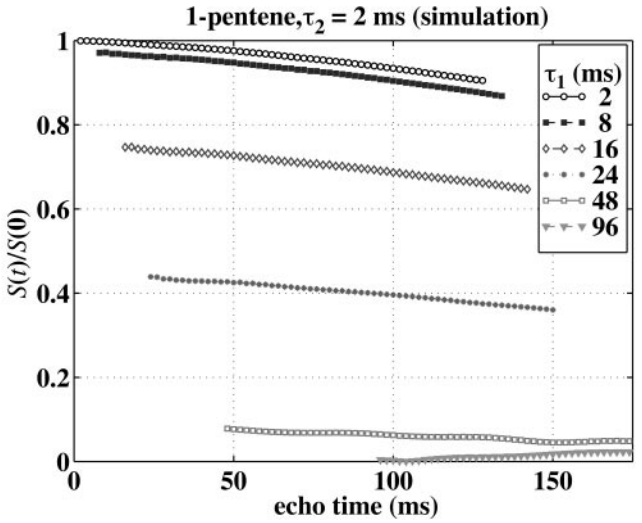

FIG. 3. Simulated DIET echo train for 1-pentene. $\tau_2 = 2$ ms, $\tau_1 = 2$ to 96 ms. The absolute value is shown and intrinsic T_2 relaxation is neglected. The topmost curve shows the echo train when $\tau_1 = \tau_2$, i.e., the CPMG version of the sequence. In this fast pulse regime, the sole effect of increasing τ_1 is to shift the entire echo train downward. The simulations support the hypothesis that when the pulse spacing is shortened in the second phase of the DIET sequence, the spin system retains the J coupling-induced signal suppression acquired before the first echo.

$$\langle \hat{I}_x(t) \rangle = \mathrm{Tr}[\hat{\rho}(t)\hat{I}_x], \qquad [1]$$

where $\hat{I}_x$ is the x component of the angular momentum operator, $\hat{\rho}(t)$ is the density matrix of the system, Tr denotes the trace, and the angle brackets denote the expected value (*12*). The equation for $\hat{\rho}$, as derived in the Appendix, is

$$\hat{\rho}(\tau_1 + n\tau_2) \propto (e^{-i/2\hat{H}\tau_2}\hat{R}_{180x}e^{-i/2\hat{H}\tau_2})^n(e^{-i/2\hat{H}\tau_1}\hat{R}_{180x}e^{-i/2\hat{H}\tau_1}) \times \hat{I}_x(e^{-i/2\hat{H}\tau_1}\hat{R}_{180x}e^{-i/2\hat{H}\tau_1})^{-1}(e^{-i/2\hat{H}\tau_2}\hat{R}_{180x}e^{-i/2\hat{H}\tau_2})^{-n}. \qquad [2]$$

The effect of T_2 relaxation is omitted, but can be included by multiplying the RHS of Eq. [2] by $\exp[-(\tau_1 + n\tau_2)/T_2]$.

The time evolution of $\hat{\rho}$ in Eq. [2] was tracked using a program written in MATLAB (Mathworks, Natick, MA). The program is based on a simulation, written to calculate $\hat{\rho}(t)$ in a CPMG sequence, that has been described previously (*9*). The parameters needed by the program to characterize each spin system are the chemical shifts of its protons and their respective J couplings. These values are used to derive the matrix representation of the Hamiltonian operator. The program can handle spin systems of arbitrary size and complexity, provided the computer has enough memory to manipulate the resulting $2^N \times 2^N$ matrices, where N is the number of spins in the system. The pulse sequence is characterized by τ_1 and τ_2 and the length of the echo train (on which there are no restrictions). All refocusing pulses are treated as ideal and produce exact 180° rotations.

In our simulations, we studied 1-pentene ($CH_3CH_2CH_2CH = CH_2$) as a model for the hydrocarbon chains found in lipids. 1-Pentene was chosen because, as a 10-spin system, it was the largest hydrocarbon chain which we could simulate (MATLAB required 100 Mb of RAM to calculate its DIET signal). The J coupling values and chemical shifts for the protons in 1-pentene were first estimated from values given in the literature for 1-hexene, 1-propene, and 1-butene (*13, 14*). These estimates were then fine-tuned by matching the theoretical spectra they produced to a high-resolution (7 T) spectrum of 1-pentene (*15*).

Experimental Methods

The DIET signal behavior of 1-pentene was also studied experimentally, along with olive oil and a solution of water doped with 0.03 mM $MnCl_2$. Olive oil was chosen for its similarity to tissue fat, while the $MnCl_2$ solution was chosen because it has no J coupling and its transverse relaxation time is similar to that of olive oil in the limit of rapid refocusing. Measurements were performed at 2.0 T on a GE Omega imaging spectrometer.

RESULTS OF SIMULATION AND PHANTOM STUDIES

Figures 3 and 4 show the results of the simulated and experimental studies, respectively, of the DIET signal for 1-pentene, where τ_2 (the second echo spacing) = 2 ms. Echo trains are shown for τ_1 values ranging from 2 to 96 ms. In Fig. 3, the absolute value of the signal, $S(t)$, is shown relative to its value immediately after the initial 90° RF pulse, $S(0)$, and

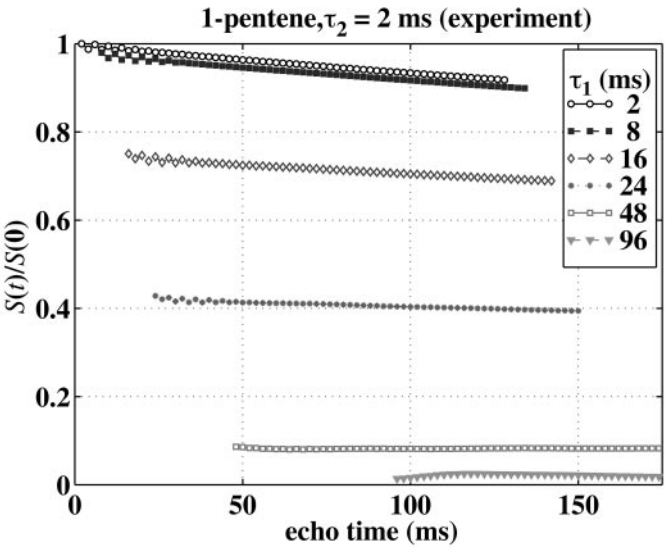

FIG. 4. Experimental DIET echo train for 1-pentene. $\tau_2 = 2$ ms, $\tau_1 = 2$ to 96 ms. The echo trains are nearly identical to those predicted numerically, indicating that J coupling is responsible for the signal suppression seen here as τ_1 increases.

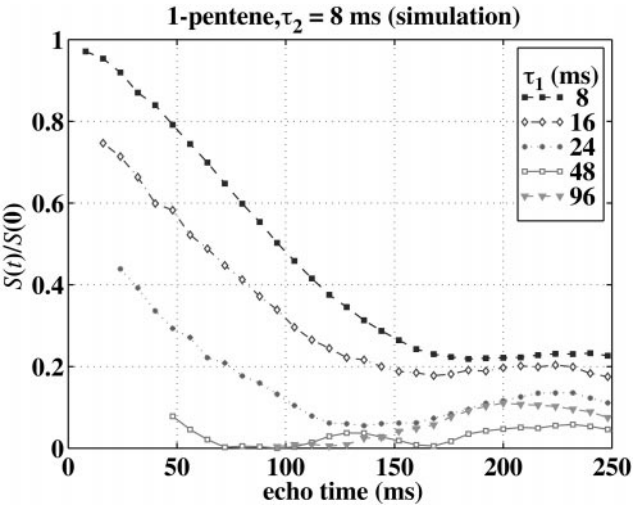

FIG. 5. Simulated DIET echo train for 1-pentene. $\tau_2 = 8$ ms, $\tau_1 = 8$ to 96 ms. In this regime, τ_2 is not fast enough to fully suppress the effects of J coupling, resulting in a greater signal modulation than was seen in Fig. 3. Again, as τ_1 increases, the signal is more fully suppressed.

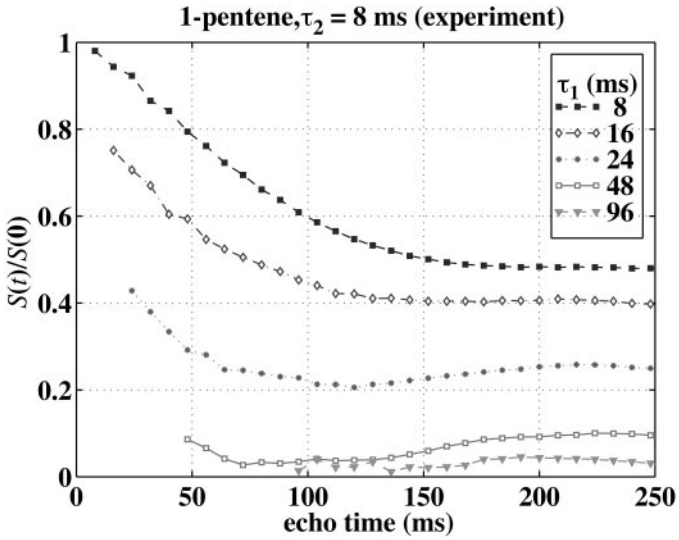

FIG. 6. Experimental DIET echo train for 1-pentene. $\tau_2 = 8$ ms, $\tau_1 = 8$ to 96 ms. The experimental echo trains show the same variations as those predicted numerically for $\tau_2 = 8$ ms; however, the amplitudes of these variations are not as pronounced.

intrinsic T_2 relaxation is omitted. In Fig. 4, the precise value of $S(0)$ is not known; therefore the signal at $t = 2$ ms is used as an approximation. The topmost curve of each figure shows the echo train when $\tau_1 = \tau_2$, i.e., the CPMG version of the sequence.

The simulated and experimental echo trains shown in Figs. 3 and 4 are in excellent agreement, establishing that the effects of J coupling are responsible for the DIET signal suppression of 1-pentene. The figures show that each echo train retains the J coupling suppression obtained during the initial τ_1 period of the sequence, and thus as τ_1 increases, the signal in the entire echo train becomes more effectively suppressed. When $\tau_1 = 48$ ms, for example, the signal decreases by over 90%. Furthermore, the echo trains show behavior approaching the time independence predicted theoretically in the Appendix, suggesting that when $\tau_2 = 2$ ms, the DIET sequence is near the fast pulse limit ($|J_{jk}|\tau_2$, $|\delta_j|\tau_2 \ll 1$) for the 1-pentene system. (Simulated echo trains where $\tau_2 = 0.5$ and 1 ms show even greater time independence.) The DIET echo trains roughly match the CPMG ($\tau_1 = \tau_2$) echo train in slope, but their overall signal is lower. This is true even for the simulated $\tau_1 = 96$ ms echo train; however, the signal in that echo train is negative, so when the absolute value is taken, the slope of the echo train becomes positive.

Figures 5 and 6 show the simulated and experimental echo trains for 1-pentene when $\tau_2 = 8$ ms. Because of the longer τ_2, the J coupling-induced signal decay is much more pronounced than when $\tau_2 = 2$ ms. Just as in Figs. 3 and 4 however, increasing τ_1 shifts the echo trains downward. Once the signal falls near zero, the echo train remains suppressed but its dependence on τ_1 becomes much less pronounced. The simulated and experimental echo trains are qualitatively very similar, but the variations in the echo trains predicted numerically are greater than those seen experimentally. It may be that in the experimental data, the effects of J coupling are slightly moderated by stimulated echoes or coherence transfer cross-relaxation phenomena, effects which are not accounted for in the simulations.

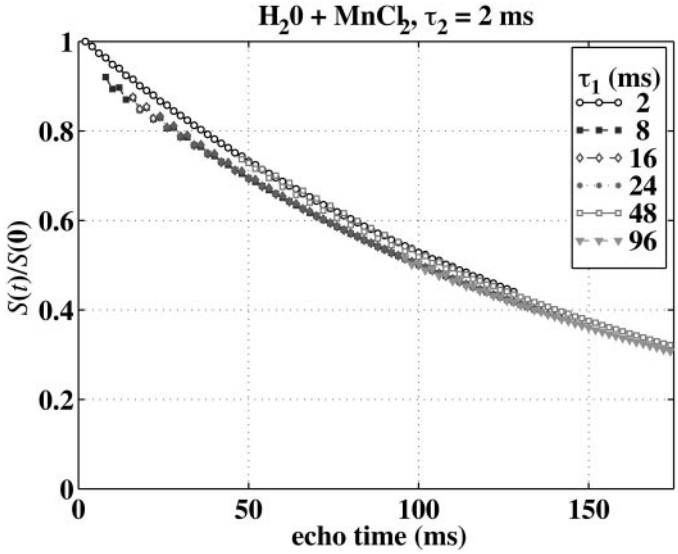

FIG. 7. Experimental DIET echo train for a solution of water doped with 0.03 mM $MnCl_2$. $\tau_2 = 2$ ms, $\tau_1 = 2$ to 96 ms. Because the solution does not contain (nonequivalent) J-coupled protons, the echo trains show normal T_2 decay and are independent of τ_1.

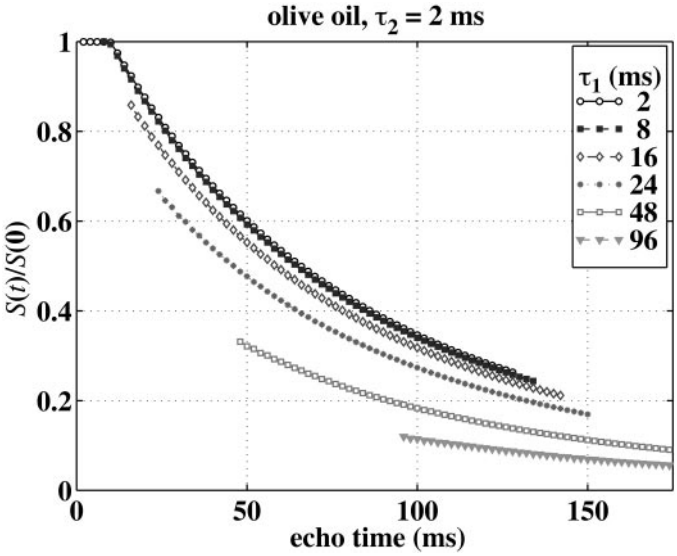

FIG. 8. Experimental DIET echotrain of olive oil. $\tau_2 = 2$ ms, $\tau_1 = 2$ to 96 ms. The dependence on τ_1 is not as dramatic as it is for 1-pentene, presumably because the molecules in olive oil contain a greater number of nearly equivalent protons.

The hypothesis that J coupling is responsible for the signal suppression observed in Fig. 4 is further supported by the DIET signal behavior seen with the $MnCl_2$ solution, as shown in Fig. 7. $\tau_2 = 2$ ms and again $S(t = 2$ ms) is used to approximate $S(0)$. The decay curves essentially overlap for all values of τ_1, as is to be expected for normal T_2 decay without J coupling.

DIET echo trains (with $\tau_2 = 2$ ms) are shown for olive oil in Fig. 8. This system again shows signal suppression with increasing τ_1, although the effect was not as dramatic as with 1-pentene. At an echo time of 48 ms, the signal of the $\tau_1 = 48$ ms echo train is roughly half that of the $\tau_1 = 2$ ms echo train. One possible explanation for the greater signal change in the 1-pentene data versus that of the olive oil data is that the majority of the oil molecule consists of chains of saturated neighboring methylene (CH_2) groups. (1-Pentene's chemical structure is $CH_3(CH_2)_2CH = CH_2$, while the chemical structure of olive oil's principal component, oleic acid, is $CH_3(CH_2)_7CH = CH(CH_2)_7CO_2H$.) Protons within long CH_2 chains have similar chemical shifts and J couplings and are therefore nearly magnetically equivalent. Thus, a greater percentage of the alkene molecule consists of spins experiencing strong J coupling effects while the longer lipid molecule has more near-equivalent spins which experience weak J coupling effects and dilute the overall signal change. In addition, the intrinsic transverse relaxation times of the protons in these molecules may be different, and are likely shorter in the larger oil chains. Thus the relative importance of decreasing the effects of coupling may be further reduced in the oil.

One aspect of Fig. 8 which is not completely understood is the higher slope of the $\tau_1 = 2$ ms echo trains relative to that of echo trains in which τ_1 is longer. One possible explanation is that the T_2 decays of 1-pentene and olive oil are multiexponential, and that in each molecule, the component which decays fastest is also the component most heavily suppressed by J coupling.

IMAGING EXPERIMENTS

The DIET scheme shown in Fig. 2 can also be incorporated into an imaging sequence by increasing the pulse spacing before the first phase encode step, as is illustrated in Fig. 9. In order to evaluate the contrast derived from this sequence, we compared images evaluated with the DIET imaging sequence to those from a conventional FSE sequence and a conventional SE sequence. Images within the thigh and the abdomen were collected using a 1.5-T GE "Signa" systems magnet. Mid-thigh images

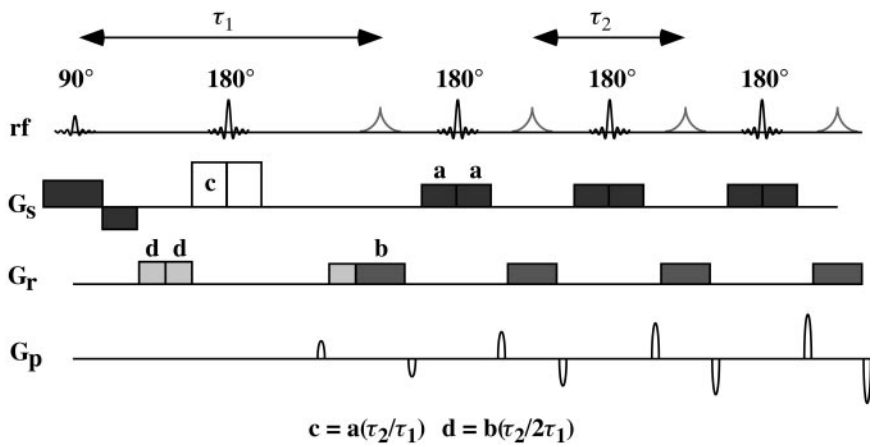

FIG. 9. The DIET Imaging Sequence. a, b, c, and d denote gradient durations (*7*).

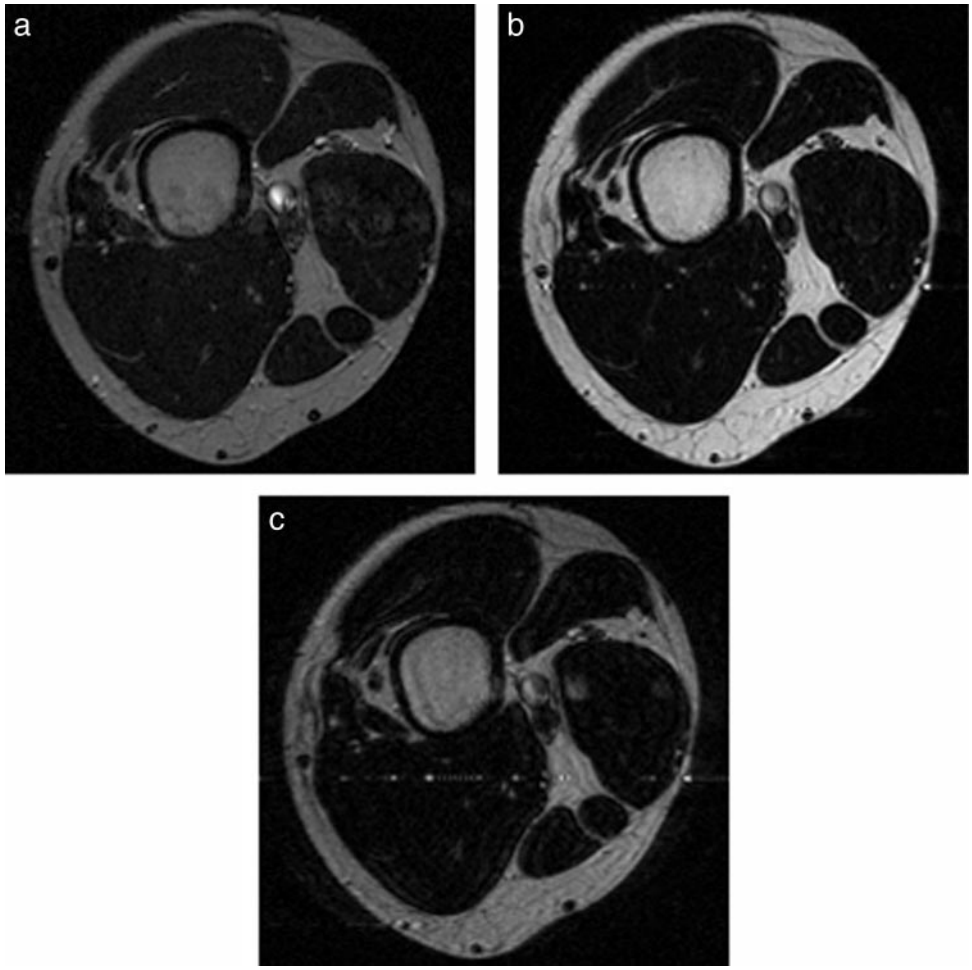

FIG. 10. Thigh images created using the (a) SE, (b) FSE, and (c) DIET imaging sequences. The TE values were 110, 112, and 108 ms, respectively. The fat signal is much less pronounced in the DIET image than in the FSE image, hence the DIET image contrast approaches that of the SE image.

were obtained using an extremity coil to contrast fat and muscle, while abdominal images were obtained with a body coil to contrast fat, muscle, and internal organs such as the kidney. The imaging parameters were: (a) SE: TE = 110 ms, TR = 2000 ms, and τ = 55 ms; (b) FSE: TE = 112 ms, TR = 3000 ms, *e*cho *t*rain *l*ength (ETL) = 16, and τ = 14 ms; and (c) DIET: TE = 108 ms, TR = 3000 ms, ETL = 16, τ_1 = 24 ms, and τ_2 = 14 ms. The FOV of each image was 20 cm. In order to make a fair comparison between images, the receiver gain was held constant for all the imaging sequences. Furthermore, to keep the effective echo times (TE) comparable between the images, the zero order phase encode of the DIET sequence was shifted to the seventh echo, rather than the eighth echo, where it occurred in the FSE sequence.

Figure 10 shows images of the upper thigh using the FSE, DIET, and SE sequences. The images are thresholded to the same levels for comparison. The contrast of the DIET image is clearly closer to that of a SE image than to that of an FSE sequence. Table 1 shows the ratio of signal from various tissues-to-fat signal, as measured in regions of interest from both the thigh and abdominal images. These ratios confirm that the contrast provided by the DIET sequence approaches that of a conventional SE sequence.

FIELD DEPENDENCE OF *J* COUPLING-INDUCED FAT SUPPRESSION

For the DIET sequence to suppress fat signal adequately, τ_1 must be long enough such that $|J_{jk}|\tau_1$ or $|\delta_{jk}|\tau_1 \geq 1$. δ is directly proportional to field strength, and thus the initial pulse spacing necessary to suppress fat will become shorter as B_0 increases. In order to qualitatively evaluate the field dependence of *J* coupling-induced fat suppression, we studied the dependence of echo amplitudes on τ for olive oil at field strengths of 0.47 and 2.0 T using a conventional CPMG

TABLE 1
Ratios of Tissue Signal to Fat Signal for FSE, DIET, and SE Images

	FSE	DIET	SE
Fat	1	1	1
Marrow	1.06	1.21	1.25
Muscle	0.12	0.16	0.15
Kidney	0.13	0.21	0.23

sequence. We recorded the echo amplitude at a fixed TE (128 ms) for a range of pulse intervals, τ. Measurements at 0.47 T were performed on a Bruker Minispec relaxometer. Figure 11 shows the field dependence of the olive oil signal. At both field strengths the signal is greatest at short pulse intervals ($\tau < 4$ ms), and similar changes are seen in going from the limit of very rapid pulsing to slow pulsing. However, as expected, at 2 T there is a more rapid decrease in signal as τ increases.

For most practical FSE imaging sequences at clinical field strengths, the pulse spacing can at best be considered to be in an intermediate regime where τ is not short enough to eliminate the fat signal entirely. For a typical FSE sequence with $\tau = 16$ ms, we can estimate from Fig. 11 the maximum amount of lipid suppression attainable by incorporating a longer initial echo into the sequence. At 2.0 T, as τ (or, for a DIET sequence, τ_1) is increased from 16 to 64 ms, the signal from olive oil is decreased by about 25%, whereas at 0.47 T the signal is decreased by over 40%. It should be noted that these estimates simply serve to show the qualitative field dependence and should not be taken as maximum estimates of suppression *in vivo* since this depends on the exact chemical nature of the coupled lipid system.

DISCUSSION

The simulations and experiments clearly support the theoretical prediction that when the pulse spacing is shortened in the second phase of the DIET sequence, the spin system retains the *J* coupling suppression acquired before the first echo. In addition, the results highlight a potential advantage of the DIET sequence over conventional CPMG-based imaging sequences: as τ_2 becomes shorter, the modulation of the echo train decreases. In imaging sequences which acquire multiple phase encodes in a single TR, a smoother echo train results in a narrower and less distorted point spread function (PSF) in the phase encode direction.

Another finding of the simulations and experiments is that for both large and small values of τ_2, the behavior of the echo train once fast pulsing begins is in many cases remarkably independent of τ_1. Therefore one can lower the initial signal of the echo train without significantly effecting its subsequent behavior. Once the faster pulsing begins, the effects of *J* coupling are removed, but the echo train's signal remains suppressed.

As discussed above, the product of the chemical shift difference(s) within the spin system and the pulse spacing, $\delta\tau$, is an important parameter which determines the degree to which *J* coupling dephases lipid signals (*6*, *9*). As $\delta\tau$ decreases, the effects of *J* coupling diminish, enhancing the lipid signal. It is apparent from our phantom experiments that even at rapid FSE pulse spacings (of order 10–20 ms), the effects of *J* coupling are still not eliminated. Thus, as new FSE sequences become available where the pulse spacing is decreased below the limits currently available on commercial systems ($\tau \cong$ 12–14 ms), the effects of *J* coupling will be more fully suppressed and lipid signal will be further enhanced. Under these conditions the DIET sequence will be particularly effective. The product $\delta\tau$ is also smaller at lower imaging field strengths, such as are found with open-bore magnets, resulting in a greater difference between SE and FSE fat signals. Once more the use of a long initial echo can greatly reduce these effects, though at lower field strengths it may be necessary to use longer τ_1 values (scaled inversely with field strength) to suppress fat signal effectively.

The length of delay before the first refocusing pulse will of course alter the sensitivity of the DIET sequence to effects other than *J* coupling, such as subject motion, flow, and diffusion through susceptibility-induced field inhomogeneities. The point spread function of the image will also be altered because of the delay before each echo is acquired.

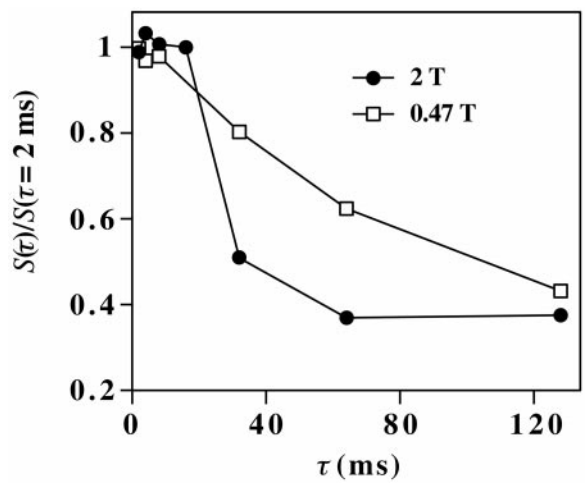

FIG. 11. Field dependence of *J* coupling induced fat suppression. The intensity of the echo at TE = 128 ms is plotted vs τ for $B_0 = 0.47$ and 2 T. The signal in each curve is normalized relative to its value when $\tau = 1$ ms. The chemical shift, δ, is larger at the higher field, and thus *J* coupling effects will be seen at shorter τ values (i.e., when $|\delta_{jk}|\tau \geq 1$).

CONCLUSIONS

We have demonstrated through density matrix theory, numerical simulations, and phantom and *in vivo* imaging experiments that the DIET sequence is an effective method of reducing lipid signal. The sequence allows one to obtain spin echo-like contrast from an FSE-type sequence. The simulations and experiments clearly support the theoretical prediction that in the limit of very fast pulsing in the second phase of the DIET sequence, the echo train becomes time independent. They also support the hypothesis that the DIET sequence should remain an effective means of fat suppression outside of the limit of short τ_2.

APPENDIX

In a standard CPMG sequence, the equation for the density matrix, $\hat{\rho}$, at the nth echo is (neglecting T_2 decay)

$$\hat{\rho}(n\tau) \propto (e^{-i/2\hat{H}\tau}\hat{R}_{180x}e^{-i/2\hat{H}\tau})^n\hat{I}_x(e^{-i/2\hat{H}\tau}\hat{R}_{180x}e^{-i/2\hat{H}\tau})^{-n}, \quad [3]$$

where τ is the spacing between 180°_x pulses, and $\hat{R}_{180x}$ is the rotation operator for the 180°_x pulse (*6*). The Hamiltonian of the system is

$$\hat{H} = -\sum_j \delta_j\hat{I}_{zj} - \sum_{j<k} J_{jk}\hat{\mathbf{I}}_j \cdot \hat{\mathbf{I}}_k, \quad [4]$$

where δ_j is the chemical shift of nucleus j with respect to the average Larmor frequency of the spins, and J_{jk} is the J coupling constant between spins j and k. $\hat{\mathbf{I}}_j$ is the angular momentum operator for the jth spin and $\hat{I}_{zj}$ is its z component. If τ is short enough that

$$|J_{jk}\tau|, |\delta_{jk}\tau| \ll 1, \text{ for all spin groups, } j, k, \quad [5]$$

then one can expand the time evolution operator, $\exp(-\frac{i}{2}\hat{H}\tau)$, to first order in a Taylor series:

$$e^{-i/2\hat{H}\tau} \approx 1 - \frac{i}{2}\hat{H}\tau = 1 + \frac{i}{2}\sum_j \delta_j\hat{I}_{zj}\tau + \frac{i}{2}\sum_{j<k} J_{jk}\hat{\mathbf{I}}_j \cdot \hat{\mathbf{I}}_k\tau. \quad [6]$$

Plugging this expansion into Eq. [3], we obtain

$$e^{-i/2\hat{H}\tau}\hat{R}_{180x}e^{-i/2\hat{H}\tau} \xrightarrow{\text{short } \tau} (1 + i\sum_j J_{jk}\hat{\mathbf{I}}_j \cdot \hat{\mathbf{I}}_k\tau)\hat{R}_{180}. \quad [7]$$

The expression on the RHS of Eq. [7] commutes with $\hat{I}_x$ and thus cancels the $(e^{-i/2\hat{H}\tau}\hat{R}_{180x}e^{-i/2\hat{H}\tau})^{-1}$ terms in Eq. [3] (*6*). Therefore, in a CPMG sequence, in the limit of $1/\tau \gg |J_{jk}|$, $|\delta_{jk}|$,

$$\hat{\rho}(n\tau) \xrightarrow{\text{short } \tau} \hat{I}_x. \quad [8]$$

For the DIET sequence, the expression equivalent to Eq. [3] is

$$\hat{\rho}(\tau_1 + n\tau_2) \propto (e^{-i/2\hat{H}\tau_2}\hat{R}_{180x}e^{-i/2\hat{H}\tau_2})^n(e^{-i/2\hat{H}\tau_1}\hat{R}_{180x}e^{-i/2\hat{H}\tau_1}) \times \hat{I}_x(e^{-i/2\hat{H}\tau_1}\hat{R}_{180x}e^{-i/2\hat{H}\tau_1})^{-1}(e^{-i/2\hat{H}\tau_2}\hat{R}_{180x}e^{-i/2\hat{H}\tau_2})^{-n}. \quad [9]$$

In the limit of fast pulsing in the second phase of the sequence (i.e., $|J_{jk}|\tau_2$ and $|\delta_j|\tau_2 \ll 1$), the outer terms can be simplified using a Taylor expansion,

$$e^{-i/2\hat{H}\tau_2}\hat{R}_{180x}e^{-i/2\hat{H}\tau_2} \xrightarrow{\text{short } \tau_2} (1 + i\sum_j J_{jk}\hat{\mathbf{I}}_j \cdot \hat{\mathbf{I}}_k\tau_2)\hat{R}_{180}. \quad [10]$$

However, because the first pulse spacing is chosen to be long enough to allow J coupling effects, i.e., $|J_{jk}|\tau_1$ or $|\delta_{jk}|\tau_1 \geq 1$, one cannot ignore higher order terms when expanding $\exp(-i\hat{H}\tau_1)$. These higher order terms contain $\hat{I}_{zj}$ operators, which do not commute with the remaining operators in Eq. [9], so the expression for $\hat{\rho}(\tau_1 + n\tau_2)$ cannot be simplified.

The expression for $\mathrm{Tr}[\hat{\rho}(t)\hat{I}_x]$ can be simplified, however, by using the relation

$$\mathrm{Tr}[\hat{\rho}\hat{I}_x] = \sum_j \langle\alpha_j|\hat{\rho}\hat{I}_x|\alpha_j\rangle, \quad [11]$$

where the $|\alpha_j\rangle$ are an orthonormal set of basis states for the system. The basis states we choose to use are the eigenstates of $\exp(-\frac{i}{2}\hat{H}\tau_1)\hat{R}_{180x}\exp(-\frac{i}{2}\hat{H}\tau_1)$, which we denote $|\xi_j\rangle$. Using Eq. [9], Eq. [11] becomes

$$\mathrm{Tr}[\hat{\rho}\hat{I}_x] = \sum_{j,k,l} \langle\xi_j|(\hat{U}_2\hat{R}\hat{U}_2)^n|\xi_k\rangle\langle\xi_k|(\hat{U}_1\hat{R}\hat{U}_1)\hat{I}_x(\hat{U}_1\hat{R}\hat{U}_1)^{-1}|\xi_l\rangle \times \langle\xi_l|(\hat{U}_2\hat{R}\hat{U}_2)^{-n}\hat{I}_x|\xi_j\rangle, \quad [12]$$

where for brevity the subscript of $\hat{R}_{180x}$ has been dropped, and $\hat{U}_1$ and $\hat{U}_2$ represent the time evolution operator, $\exp(-\frac{i}{2}\hat{H}\tau)$, at $\tau = \tau_1$ and τ_2, respectively. $\hat{U}_1\hat{R}\hat{U}_1$ is unitary, and thus has eigenvalues of the form $\exp(i\lambda_j)$ (*6*). Substituting these eigenvalues and rearranging terms, we obtain

$$\mathrm{Tr}[\hat{\rho}\hat{I}_x] = \sum_{k,l} e^{i(\lambda_k-\lambda_l)}\langle\xi_l|(\hat{U}_2\hat{R}\hat{U}_2)^{-n}\hat{I}_x(\hat{U}_2\hat{R}\hat{U}_2)^n|\xi_k\rangle\langle\xi_k|\hat{I}_x|\xi_l\rangle. \quad [13]$$

In the limit of fast pulsing in the second (τ_2) phase of the DIET sequence, one can use the Taylor expansion shown in Eq. [10]. The terms in this expansion commute with $\hat{I}_x$ so that

$$(\hat{U}_2\hat{R}\hat{U}_2)^{-n}\hat{I}_x(\hat{U}_2\hat{R}\hat{U}_2)^n \xrightarrow{\text{short } \tau_2} \hat{I}_x. \quad [14]$$

The expression for the DIET signal therefore becomes

$$S(\tau_1 + n\tau_2) \propto \mathrm{Tr}[\hat{\rho}\hat{I}_x] = \sum_{k,l} e^{i(\lambda_k - \lambda_l)} |\langle \xi_k | \hat{I}_x | \xi_l \rangle|^2. \quad [15]$$

While the values of λ_j and $|\xi_j\rangle$ depend on τ_1, there is no dependence on τ_2 or n in Eq. [15]. We have therefore demonstrated that in the limit of very fast pulsing in the second phase of the DIET sequence, the modulation of the echo train will disappear. The fat signal instead retains the suppression achieved during the first (τ_1) phase of the sequence.

ACKNOWLEDGMENT

This work was supported by Grant CA40675 from the National Institutes of Health.

REFERENCES

1. R. S. Hinks and R. M. Henkelman, Problems with organic materials for magnetic resonance imaging phantoms, *Med. Phys.* **15,** 61–63 (1988).
2. R. T. Constable, A. W. Anderson, J. Zhong, and J. C. Gore, Factors influencing contrast in fast spin-echo MR imaging, *Magn. Reson. Imaging* **10,** 497–511 (1992).
3. R. M. Henkelman, P. A. Hardy, J. E. Bishop, C. C. Poon, and D. B. Plewes, Why fat is bright in RARE and fast spin echo imaging, *J. Magn. Reson. Imaging* **2,** 533–540 (1992).
4. R. V. Mulkern, S. T. S. Wong, C. Winalski, and F. A. Jolesz, Contrast manipulation and artifact assessment of 2D and 3D RARE sequences, *Magn. Reson. Imaging* **8,** 557–566 (1990).
5. R. S. Hinks and D. Martin, Bright fat, fast spin echo, and CPMG, *in* "Proceedings, Society of Magnetic Resonance in Medicine 11th Annual Meeting," p. 4503, Berlin, 1992.
6. A. Allerhand, Analysis of Carr–Purcell spin echo NMR experiments on multiple-spin systems. I. the effect of homonuclear coupling, *J. Chem. Phys.* **44,** 1–9 (1966).
7. H. Kanazawa, H. Takai, Y. Machida, and M. Hanawa, Contrast naturalization of fast spin echo imaging: A fat reduction technique free from field inhomogeneity, *in* "Proc., SMR, 2nd Meeting, San Francisco, 1994," p. 474.
8. K. Butts, J. M. Pauly, G. H. Glover, and N. J. Pelc, Dual echo "DIET" fast spin echo imaging, *in* "Proceedings, Society of Magnetic Resonance, 3rd Scientific Meeting," Nice, France, p. 651, 1995.
9. L. A. Stables, A. W. Anderson, and J. C. Gore, The effects of *J* coupling in SE and FSE MR imaging, *in* "Proceedings, Society of Magnetic Resonance in Medicine, 12th Annual Meeting," New York, p. 1267, 1993.
10. D. Norris, P. Börnert, T. Reese, and D. Leibfritz, On the application of ultra-fast RARE experiments, *Magn. Reson. Med.* **27,** 142–164 (1992).
11. R. T. Constable, R. C. Smith, and J. C. Gore, Coupled-spin fast spin-echo MR imaging, *J. Magn. Reson. Imaging* **3,** 547–552 (1993).
12. C. P. Slichter, "Principles of Magnetic Resonance," Harper and Row, New York (1963).
13. A. A. Bothner-By and C. Naar-Colin, The proton magnetic resonance spectra of olefins. I. Propene, butene-1 and hexene-1, *J. Amer. Chem. Soc.* **83,** 231–236 (1961).
14. H. W. Quinn, J. S. McIntyre, and D. J. Peterson, Coordination compounds of olefins with anhydrous silver salts, *Can. J. Chem.* **65,** 2896–2910 (1965).
15. "The Aldrich Library of 13C and 1H FT NMR Spectra," Aldrich Chemical Co., Milwaukee, (1993).